Maximum a Posteriori Based Ocean Surface Current Inversion for Doppler Scatterometer

Weifeng Sun, *Member, IEEE*, Chen Jia, Chenqing Fan, Wen Li, Yongshou Dai, and Weimin Huang, *Senior Member, IEEE*

***Abstract*—Doppler Scatterometer (DopScat) is a new tool for sea surface wind and current fields remote sensing with rapid global coverage and wide observation swath. Existing current inversion methods for DopScat are based on maximum likelihood estimation (MLE), and its inversion accuracy cannot meet the requirements of many offshore operations. To improve the accuracy of ocean surface current measurement for DopScat, a method using prior probability distributions extracted from historical current fields is presented. First, according to the temporal correlation of ocean surface current, the minimum root mean square differences of current speed and direction are used to select the historical ocean current data correlated to those of the observation area. Next, a fitting method based on maximum likelihood is employed to fit the selected current speed and direction data to determine their prior probability distributions. Then, the obtained distributions are used to construct the cost functions of the proposed maximum a posteriori (MAP)-based current inversion method. Finally, taking the current result provided by the MLE-based current inversion method as initial guess, the cost functions of the proposed MAP-based method are optimized to obtain the final current field. Validation experiments were conducted using simulated DopScat data based on the current generated by the ocean surface current analyses real-time model, the results show that the biases of the estimated current speed and direction are better than 0.05 m/s and 15°, respectively. Compared with that of the MLE-based method, the biases are reduced by 0.16 m/s and 9°, respectively.**

***Index Terms*—Doppler scatterometer (DopScat), inversion accuracy, maximum a posteriori (MAP), ocean surface current.**

I. Introduction

OCEAN surface current finds its applications in many offshore businesses and studies, such as fishing [1], commercial shipping, global climate change analysis [2], etc. Accurate inversion of ocean surface currents over a wide area is of great significance and has attracted extensive attention [3].

Manuscript received 11 February 2023; revised 30 August 2023 and 2 October 2023; accepted 18 December 2023. Date of publication 20 December 2023; date of current version 29 December 2023. This work was supported by the National Natural Science Foundation of China under Grant 62071493 and Grant 61831010. *(Corresponding author: Weifeng Sun.)*

Weifeng Sun, Chen Jia, Wen Li, and Yongshou Dai are with the College of Oceanography and Space Informatics, China University of Petroleum (East China), Qingdao 266580, China (e-mail: sunwf@upc.edu.cn; z20160044@s.upc.edu.cn; s20160031@s.upc.edu.cn; daiys@upc.edu.cn).

Chenqing Fan is with the Remote Sensing Office of the First Institute of Oceanography, Ministry of Natural Resources, Qingdao 266061, China (e-mail: fanchenqing@fio.org.cn).

Weimin Huang is with the Faculty of Engineering and Applied Science, Memorial University of Newfoundland, St. John's, NL A1B3X5, Canada (e-mail: weimin@mun.ca).

Digital Object Identifier 10.1109/JSTARS.2023.3345148

Ocean surface current can be measured by both in-situ and remote sensing tools, as listed in Table I. Different observation methods have different measurement accuracy and application scopes. In-situ instruments [4], [5], high-frequency surface wave radar (HFSWR) [6] and X-band marine radar [7] can measure ocean current with high accuracy, but they can only provide the current field in the nearshore area. Satellite altimeters [8] can observe ocean circulation on a large scale (>200 km), but their capability of current inversion in small and medium scales is limited. Synthetic aperture radar (SAR) [9], [10] can realize global current observation with high spatial resolution, but a monostatic radar can only estimate radial current speeds rather than vector current fields. Moreover, it cannot achieve continuous observation due to its revisit period. Therefore, it is expected to develop a new sensor for estimating the vector current field with rapid global coverage.

In 2013, European Space Agency (ESA) proposed a new scatterometer system with multiview observations. Unlike the traditional scatterometry for wind field estimation [11], it was named Doppler scatterometer (DopScat) as it owns Doppler measurement capability. Compared with other ocean surface current measurement tools, such as HFSWR, spaceborne altimeter, SAR, etc., DopScat adopts a special pencil-beam rotation scanning system (see Fig. 1), thus it can achieve rapid global observation of vector currents using only a single radar. In addition, it can estimate wind and current simultaneously.

Due to the aforementioned advantages, DopScat has attracted increasing attention since Fabry et al. [12] theoretically demonstrated its feasibility. Bao et al. [13], [14] developed a simulation model for DopScat working in Ku-band and proposed a maximum likelihood estimation (MLE) method to estimate global vector currents. Their results show that the accuracies of current speed and direction retrieval are higher than 0.16 m/s and 22°, respectively. Subsequently, Rodriguez et al. [15], [16], [17] developed a Ka-band airborne DopScat for measuring the current field of the Mississippi River plume. The current speeds obtained agree well with those measured by in-situ buoy, but the retrieval accuracy of current direction is worse than 20°. A survey on "User demand index of ocean current" [18] shows that most marine services require the current speed and direction accuracies to be higher than 0.1 m/s and 20°, respectively. To further improve the ocean current inversion accuracy, Dong et al. [19] designed a Ku-Ka dual-band DopScat model and achieved a current speed accuracy of 0.05 m/s. However, the complexity of the estimation method is high. Recently, Sun

TABLE I
COMPARISONS OF OCEAN SURFACE CURRENT MEASUREMENT TOOLS

Observation method	Instrument	Application Scope	Measurement accuracy
In-situ measurement	ADCP	Rivers and lakes	0.05 m/s
	Buoy	Nearshore area	0.15 cm/s
Remote sensing measurement	HFSWR	Nearshore area (0-300 km)	0.07 m/s
	Satellite Altimeter	Large-scale ocean circulation	0.10 m/s
	SAR	Ocean surface current	0.05 m/s

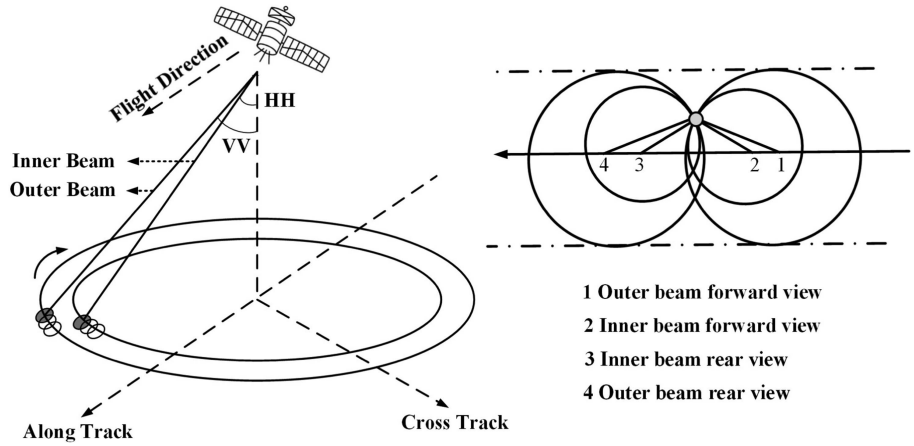

Fig. 1. Observation diagram of a pencil-beam rotation scanning system.

et al. [20] proposed a vector current velocity inversion method using optimally selected observation azimuths and obtained an estimation accuracy of 0.06 m/s for current speed, but the estimation accuracy of current direction is still not satisfactory.

Existing ocean current inversion methods for DopScat only employ real-time field data, the estimation accuracy may not satisfy the requirements of certain applications. In reality, model-generated or historical data can be used along with real-time field data to improve the accuracy of ocean dynamic parameter estimation. For example, Johannessen et al. [21] used wind direction data generated by the numerical weather prediction (NWP) model to improve wind field inversion accuracy. Elyouncha et al. [22] proposed a Bayesian-based joint method for ocean surface wind and current inversion using satellite SAR data, where the NEMO (Nucleus for European Modeling of the Ocean) model was used to provide near-surface currents and help improve the current inversion accuracy.

It is found that the change of ocean current within a period in a specific area is slow and follows some pattern, i.e., the ocean current has strong temporal correlations [23]. Therefore, the temporal characteristics can be well explored using historical data to predict present current field in an observation area, then the predicted results can be combined with those estimated from field data to further improve the ocean current results. Based on this consideration, an ocean surface current inversion method incorporating the information extracted from historical ocean current data is proposed for DopScat for the first time.

The rest of this article is organized as follows. The proposed ocean current inversion method is described in detail in Section II. In Section III, experimental results are presented and analyzed. The advantages, disadvantages, and applicability of the proposed method are discussed in Section IV. Finally, Section V concludes this article.

II. METHODOLOGY

The MLE-based method is widely used for ocean current estimation with DopScat. To further improve the inversion accuracy, the historical ocean current data correlated with those of the observation area are fitted to produce the prior probability distributions of current speed and direction. The obtained probability distributions are then incorporated with the cost function of the MLE-based method to develop an ocean current retrieval method based on the maximum a posteriori estimation (MAP) algorithm. The proposed method consists of three modules: 1) the historical ocean current data selection module, 2) the prior distribution fitting and the cost function modification module, and 3) the current field inversion module.

A. Selection of Historical Ocean Current Data

Root mean square differences (RMSDs) of current speed and direction are used to determine the preceding period in which the ocean current data have high correlation with those on present date for an observation area. As the ocean current for time t_r at present is unknown and to be estimated, the corresponding data collected at the same time t_r of the same day last year are used as reference for correlation analysis. Suppose there are M observation points within the sea surface area of interest, the RMSDs of current speed RMSD_{V_i} and current direction RMSD_{ϕ_i} at the ith $(1 \le i \le M)$ observation point are calculated using

$$\mathrm{RMSD}_{V_i} = \sqrt{\frac{\sum_{j=1}^{n} (V_{si} - V_{hj})^2}{n}} \tag{1}$$

Equation (2), shown at the bottom of the next page.
where V_{si} and ϕ_{si} denote the current speed and direction at reference time t_r for the ith observation point, V_{hj} and ϕ_{hj}

TABLE II
AVERAGE RMSDS BETWEEN REFERENCE AND CANDIDATE HISTORICAL CURRENT FIELDS FOR DIFFERENT TIME INTERVALS

Region \ Periods	Jun.	Jul.	Aug.	Jul.+Aug.	Jun.+Jul.+Aug.	Sep.
The Gulf Stream						
Speed [m/s]	0.49	0.38	0.15	0.30	0.39	0.55
Direction [°]	56.05	41.85	15.37	32.14	42.55	123.55
The Equatorial Ocean						
Speed [m/s]	0.39	0.29	0.21	0.26	0.32	0.37
Direction [°]	70.07	46.82	20.29	37.34	52.43	76.12
The North Pacific Ocean						
Speed [m/s]	0.06	0.06	0.04	0.05	0.06	0.07
Direction [°]	62.70	41.69	21.48	35.44	47.90	102.57

represent the current speed and direction at time t_r in the jth preceding day, and n is the number of selected ocean current data.

Then the average RMSD of currents of the observation area can be calculated as

$$\mathrm{RMSD}_{\mathrm{avg}} = \frac{\sum_{i=1}^{M} \mathrm{RMSD}_i}{M} \tag{3}$$

where RMSD_i denotes either RMSD_{V_i} or RMSD_{ϕ_i} for the ith observation point within the sea surface area of interest.

The candidate historical current datasets are usually selected from the data obtained several months before the observation time of the reference current in the same area. Average RMSDs $\mathrm{RMSD}_{\mathrm{avg}}$s for current speed and direction are obtained for each candidate historical current dataset. The time interval between the reference dataset and candidate historical current dataset with the minimum $\mathrm{RMSD}_{\mathrm{avg}}$ for either current speed or current direction is regarded as the preceding period to select the historical current data for present observation area. Since the estimation accuracy of current speed is better than that of current direction, $\mathrm{RMSD}_{\mathrm{avg}}$ of current speed is used for selecting the historical current data in this work.

To demonstrate how to select the historical current data, in this study, the OSCAR [24] current data from the Gulf Stream, the Equatorial region, and the North Pacific Ocean downloaded from the website https://www.esr.org/research/oscar/oscar-surface-currents/ were selected for analysis. The Gulf Stream has high current speeds ranging from 1–2 m/s due to oceanic gyre. The equatorial current is mainly affected by the northeast winds and its current speed ranges from 0.5–1 m/s. The current speed of the North Pacific Ocean is relatively small (0–0.5 m/s) all year round. It can be noted that the selected current speed data cover a wide range (0–2 m/s). Therefore, these data are good for analyzing the temporal correlation between historical current fields and those under observation.

The ocean current data collected on September 1, 2020 in these three regions were selected as references, while those collected in June, July, August 2020, and September from 2014 to 2019 were chosen as candidates. In each region, 100 observation points were selected for analysis. For each observation point, only the current data point at 8:00 A.M. of each day is provided, i.e., the data rate is one data point per day. The average RMSDs between reference and candidate current fields were calculated and shown in Table II. In Table II, "Jul. + Aug." and "Jun. + Jul. + Aug." denote that the candidate current data are from the months of July and August, and those of June, July and August, respectively. "Sep." represents the historical ocean current data collected in every September from 2014 to 2019.

It can be seen from the results in Table II that the average RMSDs obtained from the "Sep." candidates are larger than those calculated using the data from other periods, especially for current direction, indicating that the historical current data from the same months of different years are not a good choice for prior information extraction for the experimental data used here. Thus, the historical current data of every September from 2014 to 2019 are not used in the following analysis. The average RMSDs of current speed calculated using the historical current data are all less than 0.50 m/s except for the "Sep.", which shows that the historical current data from these periods have higher temporal correlations with the reference current data. It is noticed that the average RMSDs of current speed and direction have similar variation trends. For all the regions, the average RMSDs of ocean current speed and direction calculated using the current data from August are the smallest. Therefore, the ocean current data collected from each day of the preceding month are selected as the historical ocean current data for prior distribution extraction.

B. Prior Distribution Fitting and Cost Function Modification

The cost function of the MLE-based current inversion method [14] for DopScat in probability form is formulated as

$$J_{\mathrm{MLE}} = -\sum_{i=1}^{N}\left[\frac{(f_{mi}-f_{si})^2}{2V_{R_i}} + \ln\sqrt{V_{R_i}}\right] \tag{4}$$

$$\mathrm{RMSD}_{\phi_i} = \sqrt{\frac{1}{n}\sum_{j=1}^{n}(\delta\phi_{ij})^2}$$
$$\delta\phi_{ij} = \begin{cases} \phi_{si}-\phi_{hj} & 0^\circ \le |\phi_{si}-\phi_{hj}| \le 180^\circ \\ 360^\circ - |\phi_{si}-\phi_{hj}| & 180^\circ \le |\phi_{si}-\phi_{hj}| \le 360^\circ \end{cases} \tag{2}$$

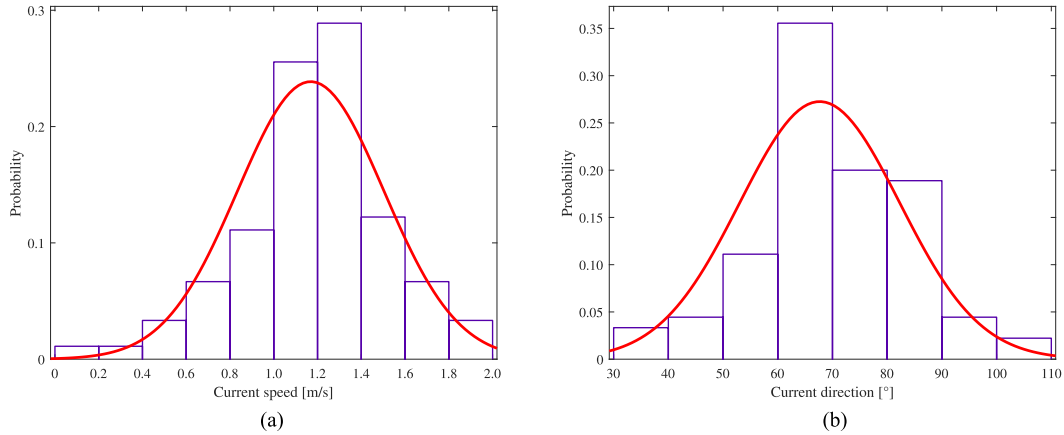

Fig. 2. Fitting results of historical ocean current data at one observation point. (a) Current speed. (b) Current direction.

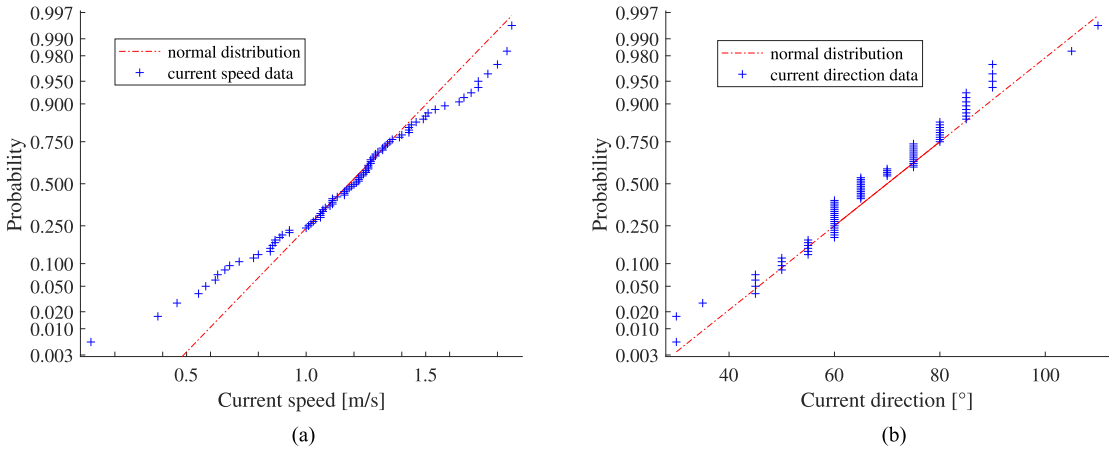

Fig. 3. Jarque Bera test results. (a) Current speed. (b) Current direction.

where N is the number of measurements for an observation point, f_{mi} denotes the Doppler frequency shift for the ith measurement, f_{si} is the Doppler frequency shift generated by the ocean surface Doppler spectrum model [25], V_{R_i} represents the variance of the residual error of the measured Doppler frequency shift.

The fitting method based on maximum likelihood [26] is applied to the selected historical ocean current data to determine the probability distributions of current speed and direction to be used as prior knowledge of the current field under observation. The fitting results of current speed and direction for one observation point are shown in Fig. 2 as an example. Similar results can be obtained for other observation points. The Jarque-Bera test was applied to the collected current speed and direction data to evaluate the goodness of fit between the probability distribution of data and normal distribution in terms of skewness and kurtosis. The current data used for probability distribution fitting contain 90 data points with current speeds ranging from 0.1–1.86 m/s and current directions varying from 30° to 110°, and the resolution of current direction is 5°. The corresponding normal probability plots are shown in Fig. 3. The red lines represent the probability plots of standard normal distributions. It can be seen that the scattered probability plots of the collected current speed and direction data fit the red lines well, and the Jarque-Bera test accepts the null hypothesis with a significance level of 5%. It should be pointed out that since the amount of current speed data within the ranges of [0.1, 1.8] m/s and [1.6, 1.86] m/s is small, the fitting results corresponding to these data slightly deviate from the standard normal distribution, as shown in Fig. 3(a). Therefore, the historical current speed and direction data involved in this study follow normal distributions. The log-likelihood functions of historical current speeds and directions are denoted as J_V and J_ϕ, respectively,

$$J_V = -\left[\frac{(V-\mu_V)^2}{2\sigma_V^2} + \ln\sigma_V + \frac{1}{2}\ln 2\pi\right] \tag{5}$$

$$J_\phi = -\left[\frac{(\phi-\mu_\phi)^2}{2\sigma_\phi^2} + \ln\sigma_\phi + \frac{1}{2}\ln 2\pi\right] \tag{6}$$

where μ_V and μ_ϕ, σ_V and σ_ϕ are the mean values and standard deviations of historical current speeds and directions, respectively. V and ϕ denote current speed and direction, respectively.

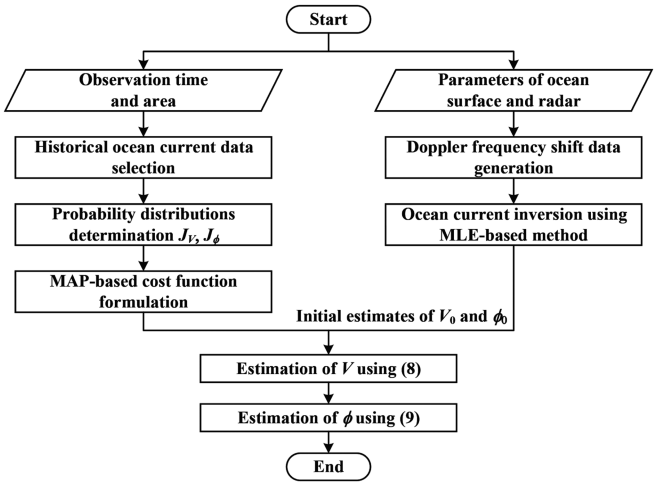

Fig. 4. Flowchart of the MAP-II based ocean current inversion method.

There are two ways to incorporate the obtained log-likelihood functions J_V and J_ϕ into the cost function (4). The first way, called the MAP-I based method, is to add J_V and J_ϕ to (4) directly, the obtained cost function can then be formulated as

$$J_{\text{MAP}} = J_{\text{MLE}} + J_V + J_\phi. \tag{7}$$

The second way, named as the MAP-II based method, is to combine J_V, J_ϕ with (4) separately to produce two cost functions J_{MAP_V} and J_{MAP_ϕ}, which can be written as

$$J_{\text{MAP}_V} = J_{\text{MLE}} + J_V \tag{8}$$

$$J_{\text{MAP}_\phi} = J_{\text{MLE}} + J_\phi. \tag{9}$$

C. Estimation of Ocean Surface Current Field

The refined ocean current speed and direction can be estimated by maximizing J_{MAP} in (7) or maximizing both J_{MAP_V} and J_{MAP_ϕ} in (8) and (9). Taking the MAP-II-based method as an example, the proposed ocean surface current inversion method is illustrated in Fig. 4 and described as follows.

Step 1: The historical current data correlated with those of the observation area are selected based on the RMSD criterion. The mean value μ_V, standard deviation σ_V of the historical current speed, the mean value μ_ϕ, standard deviation σ_ϕ of the historical current direction are calculated, then the distributions J_V of current speed and J_ϕ of current direction are determined by (5) and (6), respectively.

Step 2: The Doppler spectrum model driven by the parameters listed in Table III is used to generate the Doppler frequency shift data [14]. Then the MLE-based current inversion method is applied to obtain the initial estimates of current speed V_0 and direction ϕ_0.

Step 3: The obtained initial estimate ϕ_0 is used in the Doppler spectrum model to calculate f_{si} in (4), then the simplex search algorithm [27] is used to solve (8) to determine the final current speed V.

TABLE III
SIMULATION PARAMETERS OF DOPSCAT OCEAN CURRENT DATA

Simulation Parameters	Specifications
Satellite speed	7373 m/s
Orbital altitude	963 km
Carrier frequency	13.5 GHz
Polarization	VV
Antenna incident	60°
Observation azimuth	75°
PRF	12 kHz
Bandwidth	5 MHz

Step 4: The final current speed V is employed to update f_{si} and J_{MLE} in (4), then the simplex search algorithm is used to solve (9) to obtain the final current direction ϕ.

It should be pointed out that for the MAP-I-based method, the final current speed V and current direction ϕ can be simultaneously obtained in Step 3 by solving (7) using the simplex search algorithm.

III. EXPERIMENTS AND ANALYSIS

To evaluate the performance of the proposed MAP-I-based and MAP-II-based ocean current inversion methods, a DopScat model [13] with the parameters listed in Table III is used as the simulation platform, the ocean current, and wind data provided by the OSCAR model are used for analysis. Suppose the current field at the Gulf Stream on September 1, 2021 needs to be estimated, 222 observation points from the Gulf Stream were selected for the test. It is found that the historical ocean current data with the minimum average RMSD (i.e., high correlation) for both current speed and direction were from August, 2021, thus the historical ocean current data acquired at 8:00 A.M. each day in August (i.e., 31 days) at the Gulf Stream with a data rate of one data point per day were collected, i.e., 6882 current data points in total were used in the experiments.

The ground-truth current fields and those estimated by the MLE-based method, MAP-I based method, and MAP-II-based method are depicted in Fig. 5. The magnitude of current speed is indicated by the color bar, while the arrow shows the current direction. The correlation coefficients between the estimated and ground-truth current speed and direction are denoted as corr_v and corr_ϕ, respectively, and calculated via

$$\text{corr} = \frac{1}{M-1}\sum_{i=1}^{M}\left(\frac{U_{ti}-\mu_{u_t}}{\sigma_{u_t}}\right)\left(\frac{U_{ri}-\mu_{u_r}}{\sigma_{u_r}}\right) \tag{10}$$

where U_{ti} and U_{ri} denote the ground-truth and estimated current speed or direction.

It can be seen from Fig. 5(b)–(d) that the current speeds estimated by the MLE-based method, MAP-I-based method, and MAP-II-based method all agree well with the ground-truth values with correlation coefficients of 0.9767, 0.9919, and 0.9926, respectively. However, the current directions obtained by the three methods show a large difference. The correlation coefficient of the current direction estimated using the MAP-I-based method is similar to that obtained using the MLE-based method.

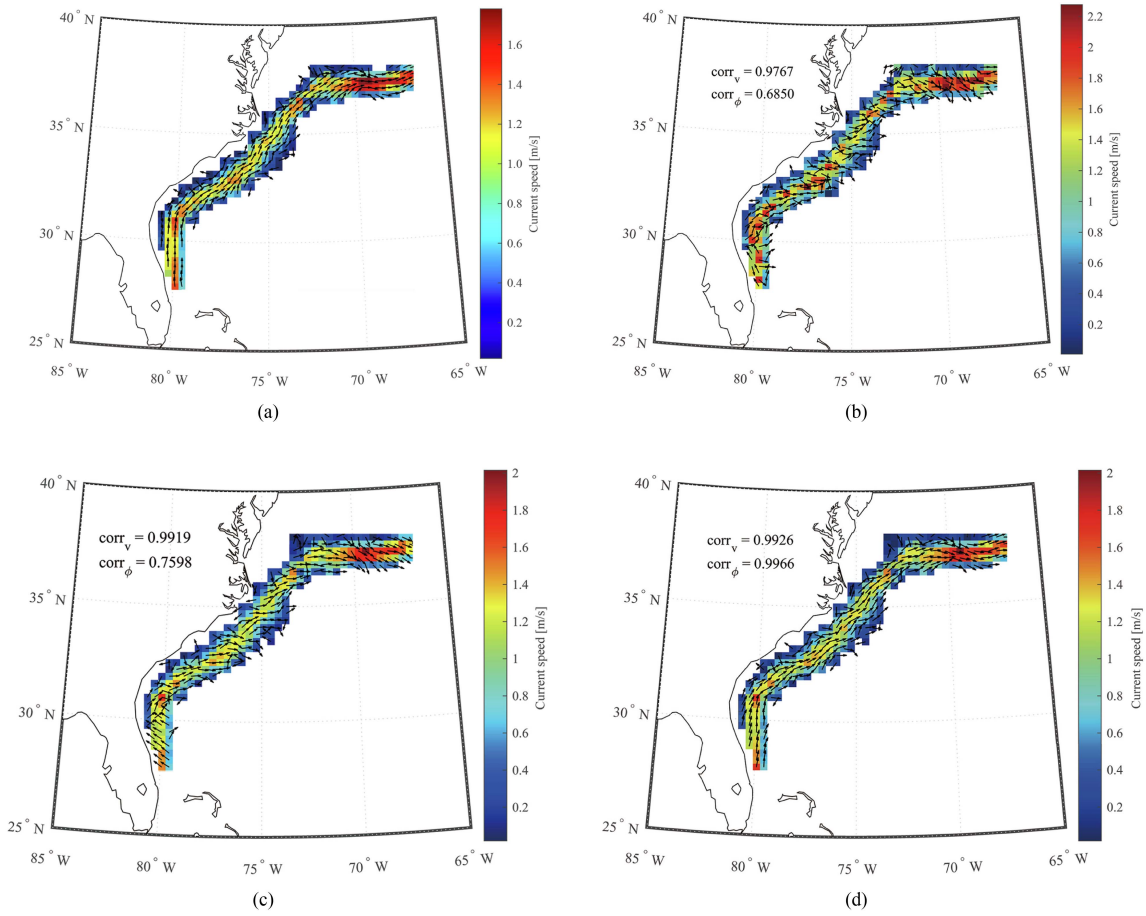

Fig. 5. Comparison of current fields. (a) Ground-truth. (b) MLE-based method. (c) MAP-I based method. (d) MAP-II based method.

In contrast, the correlation coefficient of the current direction estimated using the MAP-II-based method is 0.9966, which is 0.24 higher than that obtained using the MAP-I-based method. Thus, the proposed MAP-II-based method has a superior performance in current direction estimation.

To further illustrate the generalization of the proposed method, a total of 100 observation points were selected from different ocean areas with high speeds (1–2 m/s), moderate speeds (0.5–1 m/s), and low speeds (0–0.5 m/s), respectively. The MLE-based, MAP-I-based, and MAP-II-based current inversion methods were applied and the results were compared. The error bar graphs of the estimated current speeds and directions are shown in Fig. 6. It can be seen from Fig. 6(a) and (b) that compared with the results obtained using the MLE-based method, the current speed estimation errors of the MAP-I-based method are much lower, especially for current speeds greater than 1 m/s. However, the errors of current direction almost remain the same. It can be observed from Fig. 6(c) and (d) that compared with the current inversion results obtained using the MAP-I-based method, the current direction estimation accuracy of the MAP-II-based method is significantly improved.

Besides, current speed bias Bias_V and current direction bias Bias_ϕ are also used to evaluate the ocean surface current retrieval accuracy, which are calculated separately as

$$\text{Bias}_V = \frac{1}{M}\sum_{i=1}^{M}|V_{ri} - V_{ti}| \tag{11}$$

Equation (12), shown at the bottom of this page.
where V_{ri} and ϕ_{ri} denote the estimated current speed or direction, V_{ti} and ϕ_{ti} denote the ground-truth current speed or direction.

$$\text{Bias}_\phi = \frac{1}{M}\sum_{i=1}^{M}\Delta\phi_i$$

$$\Delta\phi_i = \begin{cases} |\phi_{ri} - \phi_{ti}| & 0^\circ \le |\phi_{ri} - \phi_{ti}| \le 180^\circ \\ 360^\circ - |\phi_{ri} - \phi_{ti}| & 180^\circ \le |\phi_{ri} - \phi_{ti}| \le 360^\circ \end{cases} \tag{12}$$

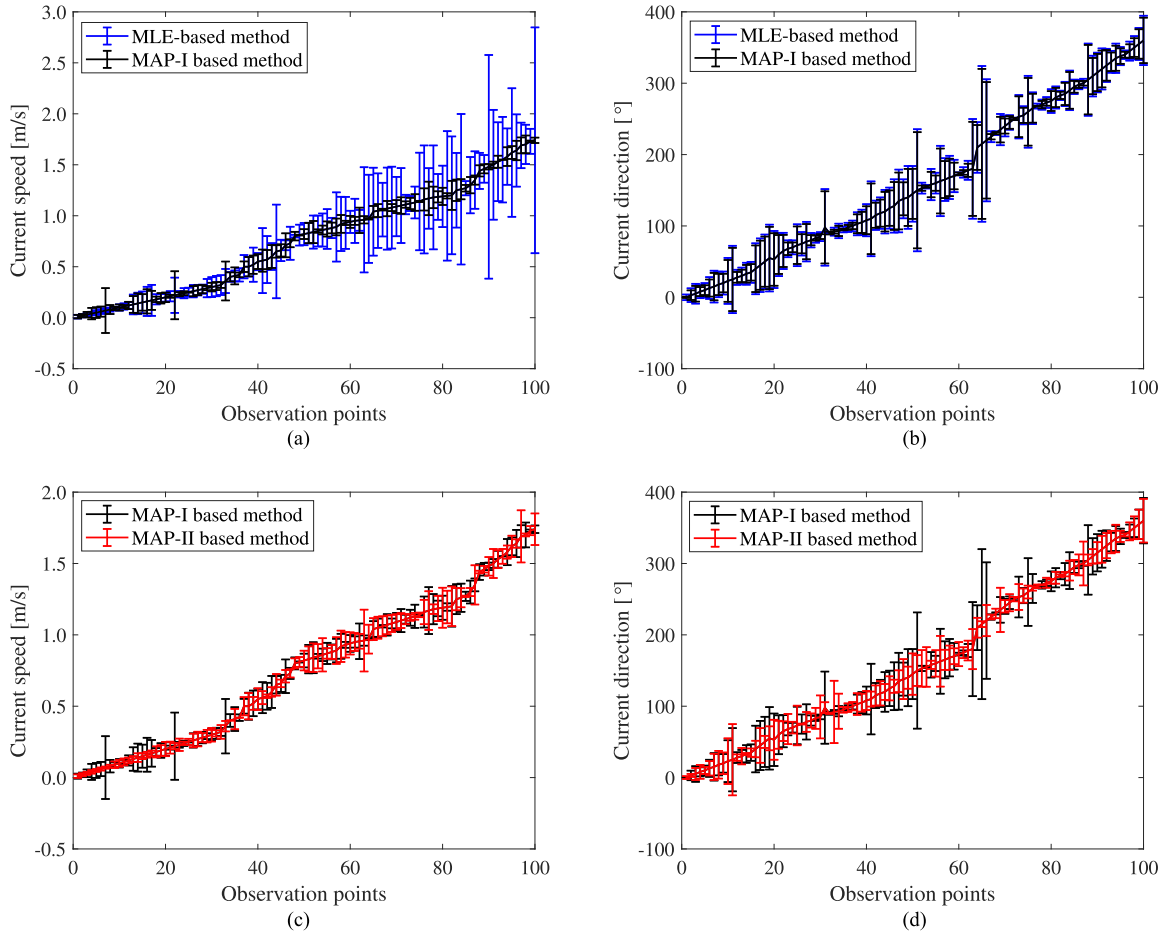

Fig. 6. Error bar graphs. (a) Current speed estimated using the MLE-method and MAP-I based method. (b) Current direction estimated using the MLE-method and MAP-I-based method. (c) Current speed estimated using the MAP-I based method and MAP-II based method. (d) Current direction estimated using the MAP-I-based method and MAP-II-based method.

TABLE IV
COMPARISON OF CURRENT INVERSION IN TERMS OF BIAS AMONG MLE, MAP-I, AND MAP-II METHODS

Method	High	Moderate	Low	Average
Current speed [m/s]				
MLE	0.38	0.19	0.06	0.21
MAP-I	0.06	0.07	0.06	0.06
MAP-II	0.07	0.07	0.03	0.05
Current direction [°]				
MLE	32.85	20.27	18.40	22.98
MAP-I	17.37	29.22	16.18	20.09
MAP-II	17.19	14.33	11.48	14.22

The biases of the estimated current speed and direction for ocean areas with different current speeds were calculated and the results are listed in Table IV. It can be found that the average bias values of current speed and direction estimated using the proposed MAP-II-based method are better than 0.05 m/s and 15°, respectively. The average bias of the current speed of the MAP-II-based method is almost the same as that of the MAP-I-based estimations, but the average bias of current direction drops by nearly 6°. Compared with the results estimated by the MLE-based method, the average bias values of current speed and direction are improved by 0.16 m/s and 9°, respectively. The bias of the estimated current speeds in the area with high current speeds is improved by nearly 82%, while the bias of the estimated current direction in the area with moderate current speeds is increased by about 50%. The above results validate that the estimation accuracy of current speed can be substantially improved by introducing prior distributions extracted from the correlated historical current data, and the current direction retrieval accuracy is greatly improved by the MAP-II-based method.

In order to verify the effectiveness of the RMSD criterion for selecting historical ocean current data, the ocean current inversion accuracy for the historical current data from different periods listed in Table II except "Sep." were analyzed using the proposed MAP-I and MAP-II ocean current inversion methods. With the current inversion results obtained using the ocean current data from September 1, 2020 as reference, the bias values were calculated and listed in Table V.

It can be seen from the results in Table V that the estimation accuracy of current speed and direction in terms of bias achieves its maximum and minimum values for the current data from

TABLE V
BIASES OF CURRENT INVERSION RESULTS FOR DIFFERENT HISTORICAL OCEAN CURRENT DATA

Method \ Periods	Jun.	Jul.	Aug.	Jul.+Aug.	Jun.+Jul.+Aug.
Current Speed [m/s]					
MAP-I	0.13	0.08	0.06	0.08	0.09
MAP-II	0.12	0.08	0.05	0.07	0.09
Current Direction [°]					
MAP-I	44.57	32.58	20.09	27.64	35.42
MAP-II	37.55	26.81	14.22	20.15	29.34

August and June 2020, respectively, and the accuracy for the data from other periods lies in between. The order is consistent with that of the RMSD results listed in Table II, which verifies the effectiveness of the RMSD criterion for selecting historical current data.

IV. DISCUSSIONS

For better illustration of the MAP-based ocean surface current inversion method, its working principle, applicability, and advantages are discussed in this section.

A. Principle of the MAP-Based Ocean Surface Current Inversion Method

The MLE-based current inversion method designed for DopScat estimates the current field only using real-time measured data. Due to the influence of system noise and model error, the estimation accuracy is relatively low. In contrast, the MAP-based current inversion method takes the MLE-based estimation result as an initial guess, which is then refined using the predicted results obtained from historical data. In other words, the current field estimated using the MAP-based method can be regarded as a weighted average of the measured current field obtained from real-time collected data and the predicted result from historical current data. The averaging process can reduce both measurement and prediction errors, thus the estimation accuracy is improved.

B. Applicability and Superiority of the MAP-Based Method

The selection and application of historical current data play an important role in the MAP-based current inversion method. In this study, the historical current field data correlated with that of the observation area are selected first according to the RMSD criterion, then the histograms of the selected historical current speed and direction data are fitted using the maximum likelihood fitting method to determine their prior probability distributions. Finally, the cost functions of MAP-based ocean current inversion are obtained by combining these prior distributions with maximum likelihood representations. It should be noted that the historical current data involved in this study all follow normal distributions. Whether this result can be applied to other current data or not needs further investigation.

Compared with the MLE-based method, the current speed retrieval accuracy of the MAP-I based method is increased by 0.15 m/s. However, the current direction estimation accuracy is only improved by 3°. It can be concluded that the accuracy improvement of current direction is more challenging. Moreover, the MAP-I-based method estimates current speed and direction simultaneously. In contrast, the MAP-II-based method employs a two-step procedure to estimate current speed and direction separately. The current speed is estimated first due to better accuracy, then it is incorporated into (9) to obtain current direction. In both the MLE-based and MAP-based methods, a Doppler spectrum model is employed to produce a Doppler frequency shift f_s with current speed and direction as input parameters, then the current speed and direction values are adjusted to make f_s approximate the measured Doppler frequency shift f_m till a preset difference is achieved, and the corresponding current speed and direction are regarded as the estimation results. Therefore, the higher the estimation accuracy of current speed is, the higher the estimation accuracy of current direction will be. As a result, the MAP-II-based method estimates the ocean current direction more accurately.

V. CONCLUSION

An MAP-based ocean surface current inversion method for DopScat is proposed to improve the current field retrieval accuracy. The contribution of this work is threefold. First, the idea that prior information of current field can be employed to increase the current inversion accuracy is proposed and validated. Second, a scheme for historical current data selection and a feasible method for prior information extraction and application are developed. Third, a two-step MAP-based method is designed to estimate current speed and direction separately, which significantly improves the current direction estimation accuracy. Experimental results demonstrate that the proposed methods perform better than existing ones.

It should be pointed out that all the DopScat data used in the experiments were simulated using ideal wind data without measurement errors. In real applications, the measurement errors of the wind field may also reduce the estimation accuracy of ocean current. Therefore, joint wind and ocean current inversion incorporating prior information is our ongoing research.

REFERENCES

[1] J. A. Hollarsmith et al., "Effects of seasonal upwelling and runoff on water chemistry and growth and survival of native and commercial oysters," *Limnology Oceanogr.*, vol. 65, no. 2, pp. 224–235, Feb. 2020.
[2] J. Blunden and D. S. Arndt, "State of the climate in 2019," *Bull. Amer. Meteorological Soc.*, vol. 101, no. 8, pp. S1–S429, Aug. 2020.

[3] A. S. Gupta, A. Stellema, G. M. Pontes, A. S. Taschetto, A. Verges, and V. Rossi, "Future changes to the upper ocean western boundary currents across two generations of climate models," *Sci. Rep.*, vol. 11, no. 1, May 2021, Art. no. 9538.
[4] P. Mercier et al., "Turbulence measurements:An assessment of acoustic Doppler current profiler accuracy in rough environment," *Ocean Eng.*, vol. 226, Apr. 2021, Art. no. 108819.
[5] J. Behrens, J. Thomas, E. Terrill, and R. Jensen, "CDIP: Maintaining a robust and reliable ocean observing buoy network," in *Proc. IEEE/OES 12th Curr. Waves Turbulence Meas.*, USA, California, 2019, pp. 1–5.
[6] L. R. Wyatt, A. Mantovanelli, M. L. Heron, M. Roughan, and C. R. Steinberg, "Assessment of surface currents measured with high-frequency phased-array radars in two regions of complex circulation," *IEEE J. Ocean. Eng.*, vol. 43, no. 2, pp. 484–505, Apr. 2018.
[7] C. Shen, W. Huang, E. W. Gill, R. Carrasco, and J. Horstmann, "An algorithm for surface current retrieval from X-band marine radar images," *Remote Sens.*, vol. 7, no. 6, pp. 7753–7767, Jun. 2015.
[8] Y. Quilfen and B. Chapron, "Ocean surface wave–current signatures from satellite altimeter measurements," *Geophys. Res. Lett.*, vol. 46, no. 1, pp. 253–261, Dec. 2018.
[9] X. Yuan et al., "Observing sea surface current by Gaofen-3 satellite along-track interferometric SAR experimental mode," *IEEE J. Sel. Top. Appl. Earth Observ. Remote Sens.*, vol. 14, no. 7, pp. 7762–7770, Jul. 2021.
[10] V. Zamparelli, F. D. Santi, A. Cucco, S. Zecchetto, G. D. Carolis, and G. Fornaro, "Surface currents derived from SAR Doppler processing: An analysis over the Naples coastal region in South Italy," *J. Mar. Sci. Eng.*, vol. 8, no. 3, Mar. 2020, Art. no. 203.
[11] Q. Feng, J. Zou, Q. Bao, and M. Lin, "Wind retrieval accuracy analysis of HY-2B microwave scatterometer," in *Proc. IEEE Int. Geosci. Remote Sens. Symp.*, Japan, Yokohama, 2019, pp. 8023–8026.
[12] P. Fabry et al., "Feasibility study of sea surface currents measurements with Doppler scatterometers," in *Proc. ESA*, 2013, pp. 1–7.
[13] Q. Bao, X. Dong, D. Zhu, S. Lang, and X. Xu, "The feasibility of ocean surface current measurement using pencil-beam rotating scatterometer," *IEEE J. Sel. Topics Appl. Earth Observ. Remote Sens.*, vol. 8, no. 7, pp. 3441–3451, Jul. 2015.
[14] Q. Bao, M. Lin, Y. Zhang, X. Dong, S. Lang, and P. Gong, "Ocean surface current inversion method for a Doppler scatterometer," *IEEE Trans. Geosci. Remote Sens.*, vol. 55, no. 11, pp. 6505–6516, Nov. 2017.
[15] E. Rodriguez et al., "Estimating ocean vector winds and currents using a ka-band pencil-beam Doppler scatterometer," *Remote Sens.*, vol. 10, no. 4, Apr. 2018, Art. no. 576.
[16] E. Rodriguez, "On the optimal design of Doppler scatterometers," *Remote Sens.*, vol. 10, no. 11, Nov. 2018, Art. no. 1765.
[17] A. Wineteer et al., "Measuring winds and currents with ka-band Doppler scatterometry: An airborne implementation and progress towards a space-borne mission," *Remote Sens.*, vol. 12, no. 6, Mar. 2020, Art. no. 1021.
[18] F. Fois, P. Hoogeboom, F. L. Chevalier, A. Stoffelen, and A. Mouche, "DopSCAT: A mission concept for simultaneous measurements of marine winds and surface currents," *J. Geophysical Res. Oceans.*, vol. 120, no. 12, pp. 7857–7879, Dec. 2015.
[19] Y. Miao, X. Dong, Q. Bao, and D. Zhu, "Perspective of a ku-ka dual-frequency scatterometer for simultaneous wide-swath ocean surface wind and current measurement," *Remote Sens.*, vol. 10, no. 7, Jul. 2018, Art. no. 1042.
[20] W. Sun, Q. Wang, W. Huang, C. Fan, and Y. Dai, "Vector current measurement using Doppler scatterometry with optimally selected observation azimuths," *Remote Sens.*, vol. 13, no. 21, Oct. 2021, Art. no. 4263.
[21] M. Portabella, A. Stoffelen, and J. A. Johannessen, "Toward an optimal inversion method for synthetic aperture radar wind retrieval," *J. Geophys. Res. Oceans*, vol. 107, no. C8, Aug. 2002, Art. no. 3086.
[22] A. Elyouncha, L. E. B. Eriksson, G. Brostrom, L. Axell, and L. H. M. Ulander, "Joint retrieval of ocean surface wind and current vectors from satellite SAR data using a Bayesian inversion method," *Remote Sens. Environ.*, vol. 260, Jul. 2021, Art. no. 112455.
[23] Y. Ashkenazy and H. Gildor, "Long-range temporal correlations of ocean surface currents," *J. Geophysical Res.*, vol. 114, no. C9, Sep. 2009, Art. no. C09009.
[24] K. Dohan, "Ocean surface currents from satellite data," *J. Geophysical Res. Oceans*, vol. 122, no. 4, pp. 2647–2651, Apr. 2017.
[25] R. Romeiser and D. R. Thompson, "Numerical study on the along-track interferometric radar imaging mechanism of oceanic surface currents," *IEEE Trans. Geosci. Remote Sens.*, vol. 38, no. 1, pp. 446–458, Jan. 2000.
[26] A. W. Bowman and A. Azzalini, *Applied Smoothing Techniques for Data Analysis*. New York, NY, USA: Oxford Univ. Press, 1997.
[27] J. C. Lagarias, J. A. Reeds, M. H. Wright, and P. E. Wright, "Convergence properties of the Nelder–Mead simplex method in low dimensions," *SIAM J. Optim.*, vol. 9, no. 1, pp. 112–147, Dec. 1998.

Weifeng Sun (Member, IEEE) received the B.Eng. degree in communication engineering and the Ph.D. degree in signal and information processing from Shandong University, Jinan, China, in 2005 and 2010, respectively.

From 2018 to 2019, he was a Visiting Scholar with the Memorial University of Newfoundland, St. John's, NL, Canada. He is currently a Professor with the College of Oceanography and Space Informatics, China University of Petroleum (East China), Qingdao, China. His research interests include marine target detection and tracking via compact high-frequency surface wave radar, image processing.

Chen Jia received the B.Eng. degree in communication engineering from Zaozhuang University, Zaozhuang, China, in 2020. She is currently working toward the M.Eng. degree in intelligent information processing with the College of Oceanography and Space Informatics, China University of Petroleum (East China), Qingdao, China.

Her research interest inlcudes ocean microwave remote sensing.

Chenqing Fan received the M.S degree in signal and information processing from the China University of Petroleum (East China), Qingdao, China, in 2009 .

He is currently an Associate Researcher with the First Institute of Oceanography, Ministry of Natural Resources, Qingdao, China. His research interests include radar altimeters, microwave radar imaging, and ocean remote sensing.

Wen Li received the B.Eng. degree in communication engineering from Linyi University, Linyi, China, in 2020. She is currently working toward the M.Eng. degree in intelligent information processing with the College of Oceanography and Space Informatics, China University of Petroleum (East China), Qingdao, China.

Her research interest includes ocean microwave remote sensing.

Yongshou Dai received the B.S. degree in production process automation from the University of Petroleum, Dongying, China, in 1986, the M.Eng. degree in computer application from Northern Jiaotong University, Beijing, China, in 1991, and the Ph.D. degree in control theory and control engineering from the University of Science and Technology Beijing, Beijing, China, in 2007.

He is currently a Professor with the College of Oceanography and Space Informatics, China University of Petroleum (East China), Qingdao, China. His research interests include seismic signal processing, marine environment monitoring, and information processing.

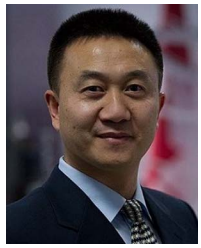

Weimin Huang (Senior Member, IEEE) received the B.S., M.S., and Ph.D. degrees in radio physics from Wuhan University, Wuhan, China, in 1995, 1997, and 2001, respectively, and the M.Eng. degree in electrical engineering from the Memorial University of Newfoundland, St. John's, NL, Canada, in 2004.

From 2008 to 2010, he was a Design Engineer with Rutter Technologies, St. John's, NL, Canada. Since 2010, he has been with the Faculty of Engineering and Applied Science, Memorial University of Newfoundland, St. John's, NL, Canada, where he is currently a Professor. He has authored or coauthored more than 260 research articles. He has edited the book *Ocean Remote Sensing Technologies: High Frequency, Marine, and GNSS-Based Radar*. His research interests include the mapping of oceanic surface parameters via high-frequency ground wave radar, X-band marine radar, synthetic aperture radar, and global navigation satellite systems.

Dr. Huang was the recipient of a Postdoctoral Fellowship from the Memorial University of Newfoundland, the Discovery Accelerator Supplements Award from NSERC in 2017, and the IEEE Geoscience and Remote Sensing Society 2019 Letters Prize Paper Award as well as some other teaching and research awards. He is also an Area Editor for the IEEE CANADIAN JOURNAL OF ELECTRICAL AND COMPUTER ENGINEERING, an Associate Editor for IEEE GEOSCIENCE AND REMOTE SENSING LETTERS, IEEE JOURNAL OF OCEANIC ENGINEERING, *Remote Sensing*, *Frontiers in Marine Science*, and is a Guest Editor for the IEEE JOURNAL OF SELECTED TOPICS IN APPLIED EARTH OBSERVATIONS AND REMOTE SENSING and five other journals. He is a Reviewer for more than 130 international journals and a Reviewer for many IEEE international conferences, such as RadarCon, International Conference on Communications, IEEE Global Communications Conference, and IEEE International Geoscience and Remote Sensing Symposium, and Oceans. From 2018 to 2021, he was a Member and Co-Chair of the Electrical and Computer Engineering Evaluation Group for Natural Sciences and Engineering Research Council of Canada Discovery Grants. He has been a Technical Program Committee Member. He is the General Co-Chair and Technical Program Co-Chair for the IEEE Oceanic Engineering Society 13th Currents, Waves, and Turbulence Measurement Workshop.